Heliyon 9 (2023) e17052

Contents lists available at ScienceDirect

Heliyon

journal homepage: www.cell.com/heliyon

Emodin attenuates high lipid-induced liver metastasis through the AKT and ERK pathways *in vitro* in breast cancer cells and in a mouse xenograft model

Feng Li [1], Xiaoyun Song [1], Xiqiu Zhou, Lili Chen, Jinzhou Zheng [*]

Longhua Hospital Affiliated to Shanghai University of Traditional Chinese Medicine, 725 Wanpingnan Road, Shanghai, 200032, China

ARTICLE INFO

Keywords:
Emodin
Liver metastasis
Breast cancer
AKT pathway
ERK pathway
Lipid synthesis

ABSTRACT

Emodin, a natural anthraquinone derivative, can inhibit lipid synthesis and breast cancer cell proliferation. We previously found that emodin decreased breast cancer liver metastasis via epithelial-to-mesenchymal transition (EMT) inhibition. However, the mechanism through which emodin affects breast cancer liver metastasis in high-fat diet-induced obese and hyperlipidemic mice has not been elucidated. Bioinformatics analysis was used to reveal the potential targets and pathways of emodin. The mouse model of liver metastasis was established by injecting breast cancer cells into the left ventricle in high-fat diet-induced obese mice. The effect of emodin on inhibiting liver metastasis of breast cancer was evaluated by animal experiments. The mechanisms through which emodin inhibits liver metastasis of breast cancer were studied by cell and molecular biological methods. Emodin reduced lipid synthesis by inhibiting the expression of triglyceride (TG) synthesis-related genes, such as fatty acid synthase (Fasn), glycerol-3-phosphate acyltransferase 1 (Gpat1), and stearoyl-CoA desaturase (Scd1), and ultimately reduced liver metastasis in breast cancer. In addition, emodin inhibited breast cancer cell proliferation and invasion through the serine/threonine kinase (AKT) signaling and extracellular-regulated protein kinase (ERK) pathways by interacting with CSNK2A1, ESR1, ESR2, PIM1 and PTP4A3. Our results indicate that emodin may have therapeutic potential in the prevention or treatment of breast cancer liver metastasis.

1. Introduction

Breast cancer is the most prevalent cancer worldwide and the leading cause of cancer death in women [1]. Hyperlipidemia, hyperglycemia, insulin resistance, and increased inflammation associated with obesity contribute to the occurrence and development of breast cancer [2]. In the United States, the sedentary lifestyle and Western-style diets increase mortality in breast cancer patients, especially among postmenopausal overweight and obese women [3,4]. In addition, obesity is also associated with an increased incidence of metastatic breast cancers [5]. Although one study suggests that steatosis inhibits breast cancer liver metastasis [6], other studies have indicated that steatosis increases breast cancer liver metastasis [7]. In addition, in metastatic liver lesions of steatotic mice, breast cancer cells could use the lipids synthesized by the surrounding hepatocytes as an energy source for tumor growth [8].

* Corresponding author.
E-mail address: zjzhssll@163.com (J. Zheng).
[1] Li F and Song X made equal contributions to this work.

https://doi.org/10.1016/j.heliyon.2023.e17052
Received 28 June 2022; Received in revised form 1 June 2023; Accepted 6 June 2023
Available online 7 June 2023

This is consistent with the relocation of lipids from adipocytes to cancer cells to promote growth [9]. In fact, proliferating cancer cells preferentially utilize exogenous fatty acids as their membrane lipid sources [10]. Therefore, steatosis promotes liver metastasis of breast cancer by providing lipid products to the tumor as an energy source [11]. In addition, free fatty acids (FFAs) increase cell proliferation and aggressiveness in breast cancer cells by regulating p70 ribosomal protein S6 kinase (P70S6 K), AKT, and ERK1/ERK2 gene expression in the mammalian target of rapamycin (mTOR) signaling and phosphatidylinositol 3 kinase (PI3K) pathways [12].

Emodin, a natural anthraquinone derivative, is an active ingredient of many traditional Chinese herbs, including *Rheum palmatum*, *Polygonum cuspidatum*, and *Aloe vera* [13]. Previous studies have reported that emodin possesses a variety of pharmacological effects, such as antiviral, antimicrobial, antidiabetic, antihyperlipidemic, neuroprotective and hepatoprotective effects [13]. Emodin activates adenosine 5′-monophosphate (AMP)-activated protein kinase (AMPK) and peroxisome proliferator-activated receptor γ (PPAR-γ) signaling in adipocytes, which suggests that it may be a potential drug candidate for the treatment of type 2 diabetes, hyperlipidemia, and other obesity-related metabolic diseases [14]. Indeed, emodin alleviates high levels of lipids in serum and liver in obese mice induced by a high-fat diet via sterol-regulatory element-binding protein 1 (SREBP-1) and SREBP-2 downregulation [15]. Emodin inhibits glucose production by suppressing the expression of key gluconeogenic genes, enhances glucose transporter 4 (GLUT4) translocation and glucose uptake into myotubes, and thus decreases fasting plasma glucose (FBG) levels and improves glucose tolerance *in vivo* through the AMPK pathway [16]. Emodin inhibits the lipid core area and the lipid-to-collagen content ratio in plaques via regulation of granulocyte-macrophage colony-stimulating factor (GM-CSF), matrix metallopeptidase 9 (MMP-9) and PPAR-γ in apoE-deficient mice [17]. It also alleviates liver inflammation induced by lipopolysaccharides in hyperlipidemic mice [18]. Additionally, emodin attenuates hepatic steatosis by inhibiting SREBP1 activity through the AMPK and mTOR-p70S6K signaling pathways in high-fat diet-fed rats [19]. In addition, emodin induces breast cell apoptosis and inhibits breast cancer cell proliferation through ERα inhibition [20,21]. Emodin also attenuates cancer cell metastasis and angiogenesis both *in vitro* and *in vivo* via MMPs and vascular endothelial growth factor receptor 2 (VEGFR2) inhibition, which may be associated with the downregulation of Runx2 transcriptional activity [22]. We previously found that emodin decreased breast cancer liver metastasis via EMT inhibition through the antagonism of *C*C-chemokine ligand 5 (CCL5) secreted from adipocytes in mice [23]. However, it was not sufficient to evaluate the efficacy of emodin in inhibiting liver metastasis of breast cancer only through pathological diagnosis. In addition, in the liver metastasis of breast cancer, there is not only an interaction between cancer cells and adipocytes but also interactions between cancer cells and other cells, such as hepatocytes, immune cells and cancer-associated fibroblasts [24–26]. In addition, the molecular mechanism and regulation of lipid metabolism in the microenvironment of breast cancer cell liver metastasis remain unelucidated. Therefore, the present investigation aimed to clarify the mechanism underlying the inhibition of emodin on liver metastasis of breast cancer cells in the condition of high-fat diet-induced obesity.

2. Materials and methods

2.1. Materials

DMEM and fetal bovine serum (FBS) were purchased from Gibco (Grand Island, NE, USA). Dimethyl sulfoxide (DMSO), diethylpyrocarbonate (DEPC), and propidium iodide (PI) were obtained from Sinopharm Group Co. Ltd. (Shanghai, China). The cell counting kit-8 (CCK-8) kit was purchased from Dojindo Molecular Technologies (Kumamoto, Japan). Antibodies for detecting ERK1/2, phospho-ERK1/2, AKT, phospho-AKT, p38 MAPK, phospho-p38 MAPK, and β-actin were purchased from Cell Signaling Technology (Boston, MA, USA). All other chemicals were purchased from Sigma–Aldrich (St. Louis, MO, USA) unless otherwise indicated.

2.2. Cells and cell culture

Human breast cancer MBA-MB-231 cells and HepG2 hepatoma cells were purchased from the Shanghai Institute of Cell Biology, Chinese Academy of Sciences (Shanghai, China). MDA-MB-231 cells labeled with luciferase were a kind gift from Professor Sheng Liu of Longhua Hospital. Cells were cultured in DMEM (10% FBS) and 40 mg/ml gentamicin and maintained at 37 °C in a humidified atmosphere containing 5% CO2. After 48 h, 50 μM emodin was added to the cell supernatant at 37 °C.

To examine the effect of high fat on breast cancer cells, the cells were incubated with liver homogenate from obese mice, and then the cell function was determined. The liver homogenate of normal mice was employed in the control group. Frozen liver was added to a 10-fold volume of ice-cold PBS and homogenized by a tissue homogenizer. The parameters were as follows: 65 Hz, three times for 60 s each. Then, the supernatant was harvested for cell culture.

2.3. CCK-8 assay

Cell viability was determined using a CCK-8 kit by measuring the absorbance at 450 nm with a microplate reader (Synergy 2 Multi-Mode Microplate Reader, BioTek, Winooski, VT, USA) and was expressed as a percentage of the control level according to our previous work [23].

2.4. Colony formation assay

Cells were seeded in 6-well plates at a density of 500 cells per well, and after 10 days, colonies with a diameter of >0.05 mm were counted according to our previous work [23].

2.5. Lipid determination

FFA, total cholesterol (TC), triglyceride (TG), low-density lipoprotein cholesterol (LDL-C), and high-density lipoprotein cholesterol (HDL-C) quantification kits were obtained from Abcam (Cambridge, UK). Frozen liver tissue (100 mg) was cut up, mixed with 1.2 ml of a 1:1 solution of acetone:absolute ethanol, and homogenized twice for 60 s each at 65 Hz using a tissue homogenizer. After the liver tissue was completely homogenized, it was placed in the refrigerator at 4 °C overnight. After standing overnight, the liver homogenate was centrifuged at 3000 rpm at 4 °C for 15 min, and the supernatant was harvested for determination. Lipid determination was performed according to the kit instructions.

2.6. Oral glucose tolerance test (OGTT) assay

After 6 h of fasting, the mice were given 2 g/kg glucose by gavage. Blood glucose was recorded at 0, 15, 30, 60, 90, and 120 min after glucose administration. Blood glucose was monitored by the LifeScan OneTouch Verio blood glucose meter system (LifeScan IP Holdings, LLC., California, CA, USA).

2.7. Homeostasis model assessment insulin resistance (HOMA-IR) assay

After 6 h of fasting, the mice were killed under anesthesia at the end of the treatment. The liver was taken for lipid determination and polymerase chain reaction (PCR). Blood was collected for glucose and insulin determination. Insulin was determined with a mouse insulin ELISA kit (Abcam, Cambridge, USA) according to the kit instructions. HOMA-IR was calculated by the following formula: HOMA-IR = insulin × FPG/22.5.

2.8. Determination of de novo synthesis of fatty acids and cholesterol

Human hepatocyte HepG2 cells were used for the *de novo* synthesis of fatty acids and cholesterol according to a previous study [27]. Briefly, cells were seeded at 400,000/ml in a 6-well plate and cultured overnight to allow them to adhere. Different concentrations of emodin or vehicle were added to the cells and cultured for 20 h. Detection was performed using radioactive 14C-labeled acetic acid as a substrate by a liquid scintillator (PerkinElmer, Waltham Massachusetts, USA).

2.9. Quantitative reverse transcription PCR (RT–qPCR)

RT–qPCR was performed to quantify the mRNA expression levels of lipid synthesis and metabolism genes, which were calculated by the $2^{\Delta CT}$ method according to our previous work [23]. Sequence and primer information is shown in Supplementary Table 1.

2.10. Western blotting and relative quantitative Western blot analysis

Western blotting was carried out as described in our previous work [23]. Equal amounts of protein (20 μg) were loaded. ImageJ (version: 1.51) was used for the relative quantitative analysis of bands on the blots.

2.11. Wound healing assay

Wound healing assays were performed in our previous work [28]. The migration distance was normalized to the LFD vehicle group.

2.12. Transwell assay

Transwell assays were performed according to our previous work [28]. The number of invasive cells was normalized to the LFD vehicle group.

2.13. Fluorescence imaging in vivo

Fluorescence imaging was carried out according to our previous study [29]. Briefly, animals were imaged using an IVIS Lumina II *in vivo* imaging system (Caliper Life Sciences, Boston, USA) at the end of treatment by following the manufacturer's recommended procedures and settings. We focused on fluorescence signals in the livers.

2.14. Bioinformatics analysis

DrugBank (https://go.drugbank.com/) and Therapeutic Target Database (TTD) (http://db.idrblab.net/ttd/) were used to identify the potential targets of emodin. REACTOME (REAC), Gene Ontology (GO), and Kyoto Encyclopedia of Genes and Genomes (KEGG) enrichment analyses were performed with REACTOME (https://reactome.org/), g:Profiler (https://biit.cs.ut.ee/gprofiler/gost), and WebGestalt (http://www.webgestalt.org/) using the candidate targets (Supplementary Table 2) as described previously [30]. Protein–protein interactions (PPIs), interactions of transcription factor (TF)-miRNAs, and signaling pathways were carried out with

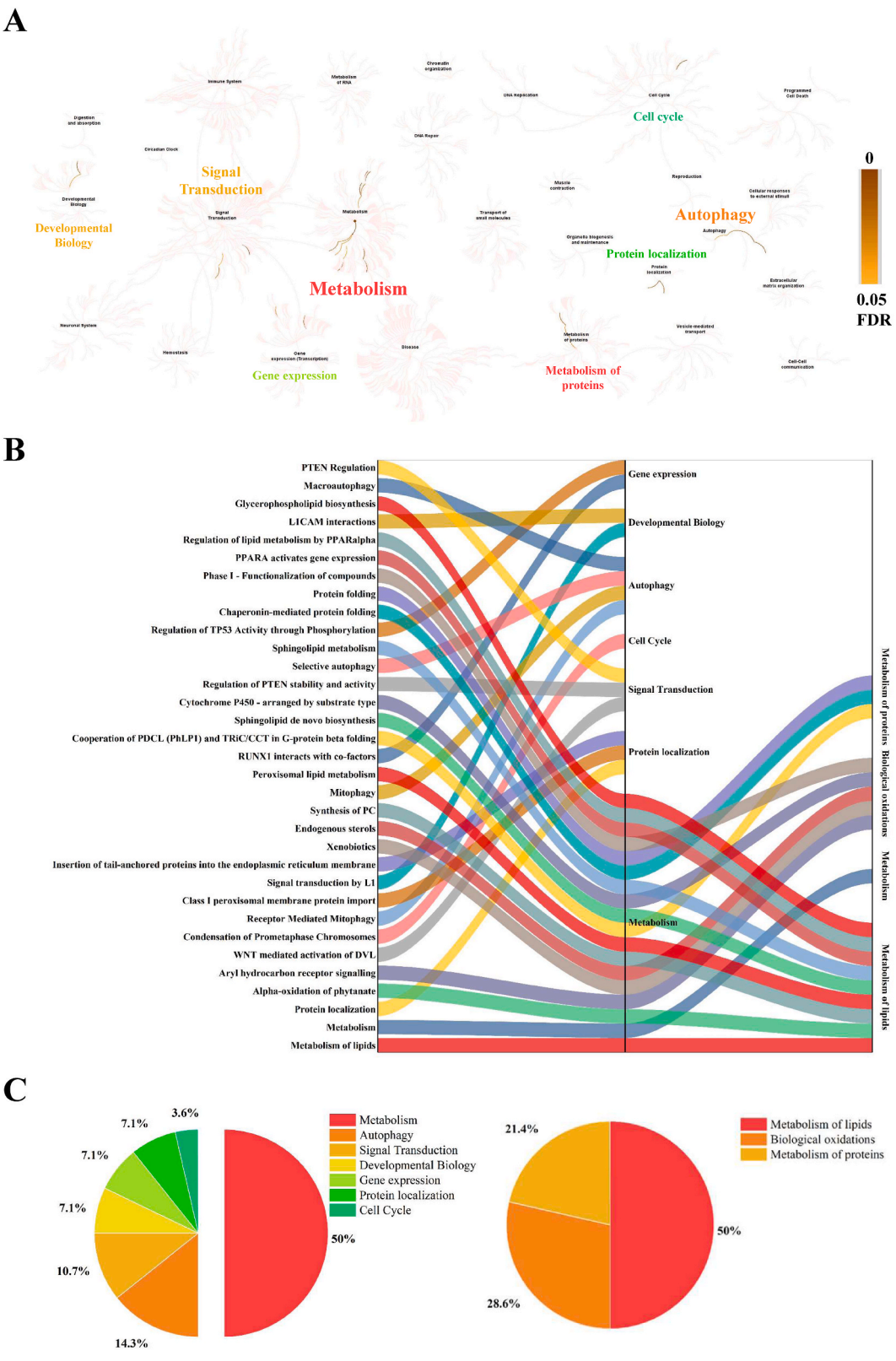

Fig. 1. Results of Reactome enrichment. (A) Overview diagram. The font size and color are consistent with figure C. (B) Sankey's diagram of the enrichment pathways and their categories. (C) Pie chart of the enrichment analysis results. (For interpretation of the references to color in this figure legend, the reader is referred to the Web version of this article.)

NetworkAnalyst (https://www.networkanalyst.ca/) using the candidate targets (Supplementary Table 2) as described in previous work [30].

2.15. Molecular docking

The molecular docking analysis was carried out using UCSF Chimera (Version 1.16) and AutoDock Vina (Version 1.12) as described in a previous study [31]. In brief, the PDB structure of the candidate protein was loaded using UCSF Chimera. The candidate compound was imported after protein minimization, and binding was analyzed by AutoDock Vina. Finally, the binding affinity was calculated. The candidate target proteins of emodin were obtained by Swiss Target Prediction (http://www.swisstargetprediction.ch/).

2.16. Animals and xenograft model procedure

Female nude (BALB/c nu/nu) mice (20 ± 2 g) were obtained from Shanghai Lingchang Biotechnology Co., Ltd. And housed in a temperature-controlled (24 ± 2 °C) room with a regular 12-h light/dark cycle. After one week of acclimatization in a specific pathogen-free (SPF) environment, 20 mice were fed a high-fat diet (HFD) using a rodent diet with 60% kcal from fat (D12492, Research Diets Inc., USA), while 12 mice were fed standard chow (LFD). HFD-induced obese mice were chosen as those with a bodyweight >20%

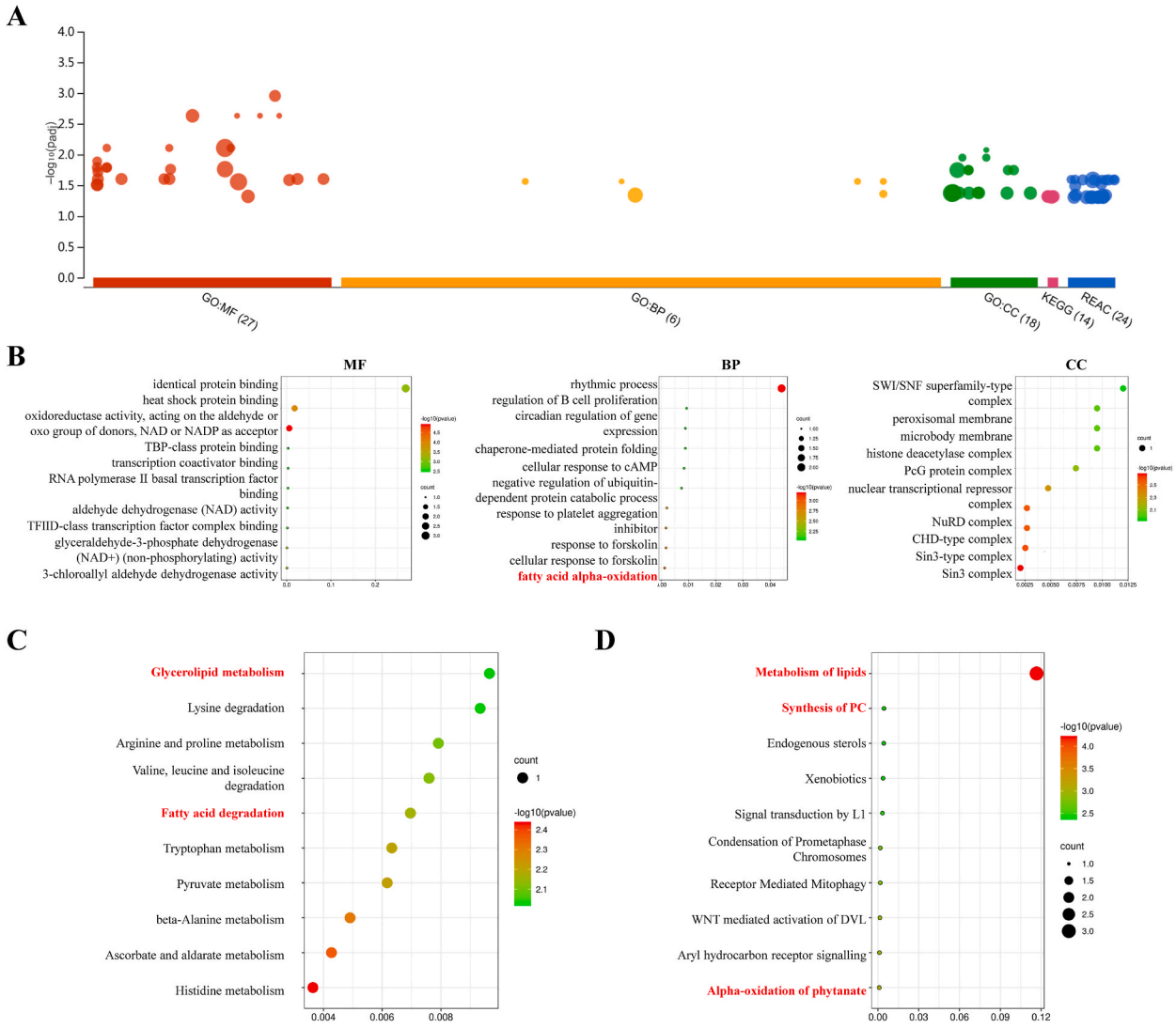

Fig. 2. Results of GO, KEGG and Reactome enrichment analyses. (A) The overview results of enrichment were analyzed by g:Profiler. (B) Top 10 terms in GO enrichment pathways by WebGestalt. (C) Top 10 terms in KEGG enrichment pathways by WebGestalt. (D) Top 10 terms in REAC enrichment pathways by WebGestalt. Pathways of lipid metabolism are highlighted in red. (For interpretation of the references to color in this figure legend, the reader is referred to the Web version of this article.)

of LFD-fed mice after 8 weeks of HFD administration and were used for the following experiments. Finally, they were divided into 4 groups according to their weight (n = 6/group). All animals had free access to water and food until the day before the experiment. All experiments were performed according to the national regulations for animal experimentation and were approved by the Institutional Animal Care and Use Committee (IACUC) of Longhua Hospital with approval number 2019-N009.

Mice were given a left ventricular injection of luciferase-labeled MDA-MB-231 cells (4.0×10^6 cells/mouse) after anesthesia with pentobarbital sodium (50 mg/kg) intravenous injection. The mice received emodin (400 mg/kg, p. o., q. d.) or vehicle for 4 weeks. The dose of emodin (Emo) was based on our previous work [23]. At the end of treatment, breast cancer cell metastasis was assessed by *in vivo* fluorescence imaging. Mice were sacrificed at the end of treatment, and metastatic liver lesions were observed by fluorescence imaging in tissues that had been collected and stored at −80 °C. The vehicle (Veh) group received an equal volume of PBS.

2.17. Statistical analysis

All results are presented as the mean ± standard deviation. Two-tailed analysis of variance (ANOVA) followed by Dunnett's post hoc test and Fisher's test were used to determine the statistical significance. A p value or false discovery rate (FDR) < 0.05 was considered significant.

3. Results

3.1. Emodin regulated lipid metabolism pathways

To explore the potential signaling pathways regulated by emodin, Reactome enrichment analysis was carried out using the candidate targets (Supplementary Table 2). Fifty-six signaling pathways were acquired via Reactome enrichment analysis, as shown in Fig. 1A. Among them, 33 pathways changed significantly with an FDR value < 0.05 (Fig. 1B). Metabolism was the major pathway identified through further classification analysis (Fig. 1C). Among these pathways, the metabolism of lipids was the main pathway, for example, alpha-oxidation of phytanate, synthesis of PC, peroxisomal lipid metabolism, sphingolipid *de novo* biosynthesis, sphingolipid metabolism, PPARα activation of gene expression, regulation of lipid metabolism by PPARα, and glycerophospholipid biosynthesis. Additionally, biological oxidation and metabolism of proteins were also enriched in the metabolism category (Fig. 1C). In addition, many autophagy-associated pathways were enriched, such as receptor-mediated mitophagy, selective autophagy and macroautophagy.

GO, KEGG, and Reactome enrichment analyses were then performed with g:Profiler. A large number of signaling pathways were enriched by g:Profiler (Fig. 2A). To reveal the relevant information of these pathways, WebGestalt analysis was subsequently carried out. There were 24, 86, and 17 terms in GO MF, BP and CC enrichment. In addition, 20 and 36 pathways were enriched based on the KEGG and Reactome enrichment analyses. Among the top 10 terms, metabolism of lipids was the dominant pathway and included fatty acid alpha-oxidation, fatty acid degradation, glycerolipid metabolism, alpha-oxidation of phytanate, and synthesis of PC (Fig. 2B–D).

3.2. Emodin activated the AKT and ERK1/2 pathways via CSNK2A1 (CK2α)

Interactions among proteins, TF-miRNAs, or signaling pathways were analyzed by NetworkAnalyst. In the PPIs, CSNK2A1 (CK2α), AHR, and ALDH3A2 interacted with other proteins, such as UBC, BRCA1, IL8, FOS, HSP90AA1, GTF2F1, AIP, SRC, RELA, and MME (Fig. 3A). miRNAs, such as hsa-miR-124, hsa-miR-125 b, hsa-miR-137, hsa-miR-141, and hsa-miR-142–5p, together with many TFs, for example, Max, EGR1, SP1, NFKB1, and AIP, regulated the expression of AHR, ALDH3A2 and CK2α (Fig. 3B). Additionally, CK2α

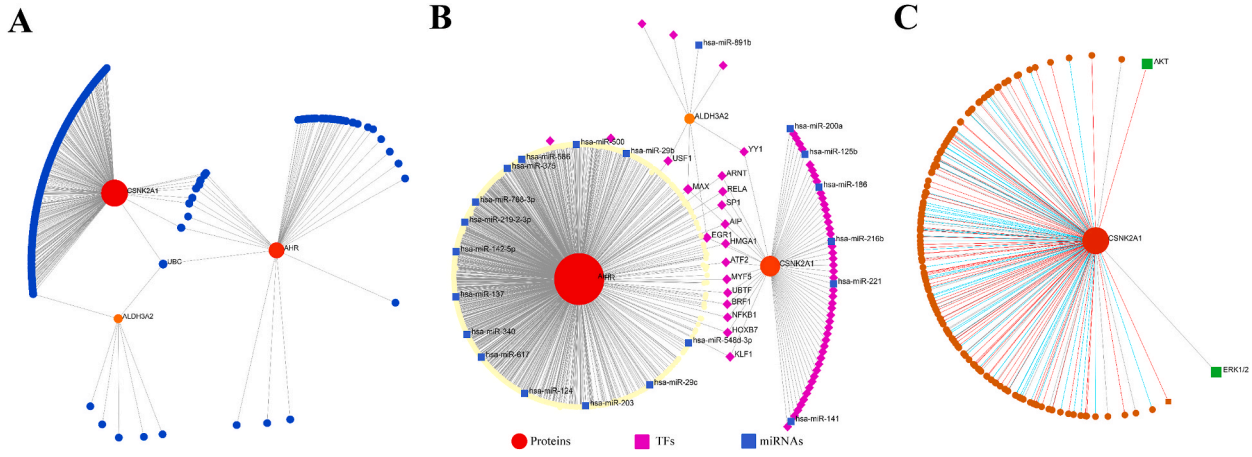

Fig. 3. PPIs and interactions of TF-miRNAs by NetworkAnalyst analysis. (A) PPIs. (B) TF-miRNA interactions. (C) Signaling pathway interactions.

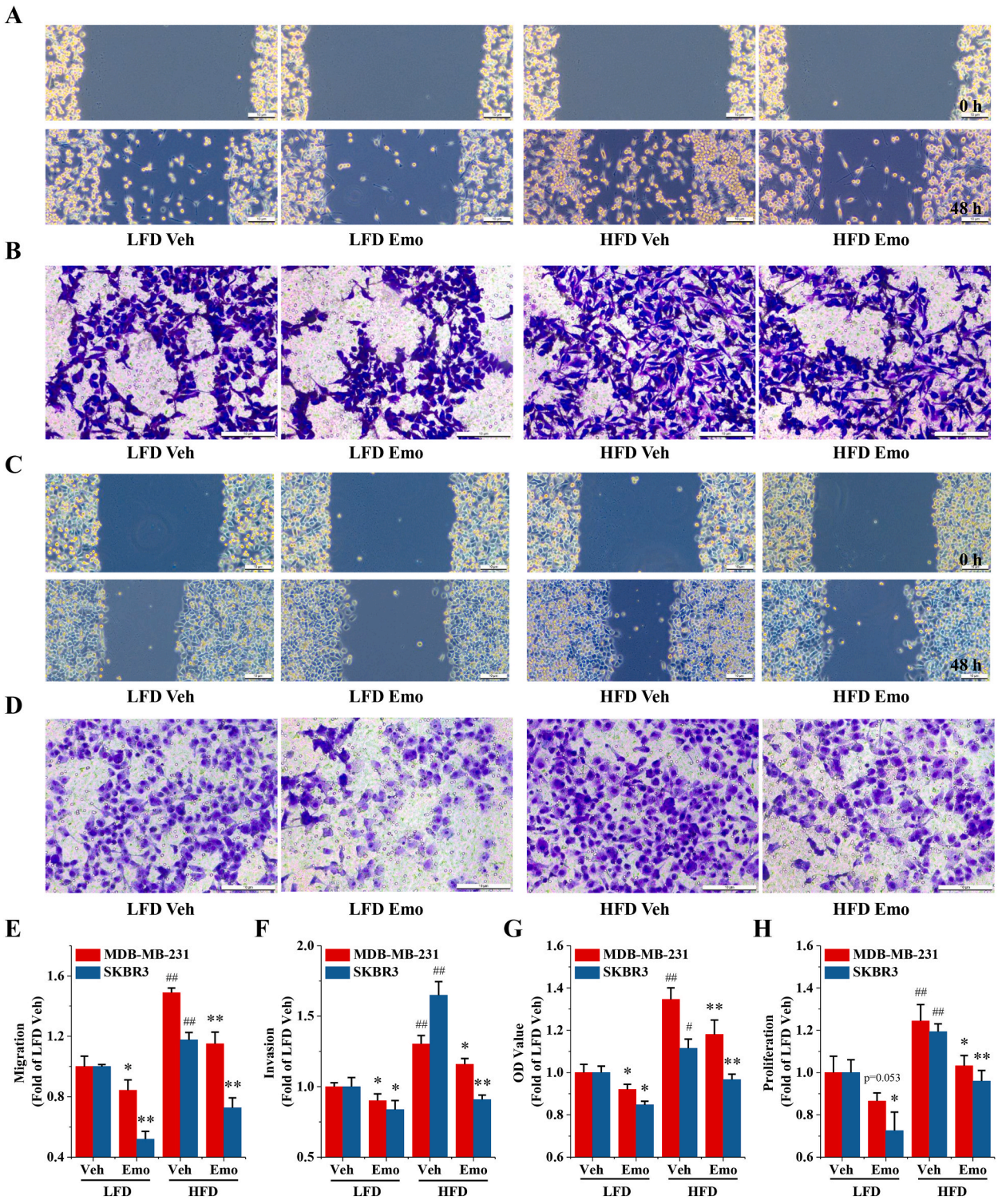

Fig. 4. Emodin attenuated the high potential malignancy of cancer cells coincubated with HFD liver homogenate extract. After the animals were sacrificed by anesthesia and bled, the mouse livers were harvested, and liver homogenates were prepared. Homogenates from the same treatment groups were mixed for subsequent cell experiments. For details of the determination, please refer to the Methods section. Data are shown as means ± SDs (n = 3). *P < 0.05 and **P < 0.01 compared to the corresponding vehicle group. $^{\#}$P < 0.05 and $^{\#\#}$P < 0.01 compared to the LFD Veh group. Three biological replicates were used for each treatment group. Emodin inhibited cancer cell migration based on wound healing assays in MDA-MB-231 cells (A/E) and SKBR3 cells (C/E) and invasion as determined by transwell invasion assays in MDA-MB-231 cells (B/F) and SKBR3 cells (D/F). Emodin reduced tumor cell activity, as shown by CCK-8 analysis (G), and proliferation, as shown by a colony formation assay (H).

activated the AKT and ERK1/2 pathways (Fig. 3C).

3.3. Emodin attenuated the high potential malignancy of breast cancer cells

To probe the effects of emodin on breast cancer cells, MDA-MB-231 and SKBR3 cells were coincubated with liver homogenate extracts from HFD or LFD mice. HFD liver homogenate extracts significantly accelerated cancer cell growth, migration, and invasion (Fig. 4). Interestingly, emodin reversed the cell migration and invasion of breast cancer cells induced by incubation with HFD liver homogenate (Fig. 4A–F). Additionally, emodin significantly reduced cell proliferation and activity in breast cancer cells (Fig. 4G/H).

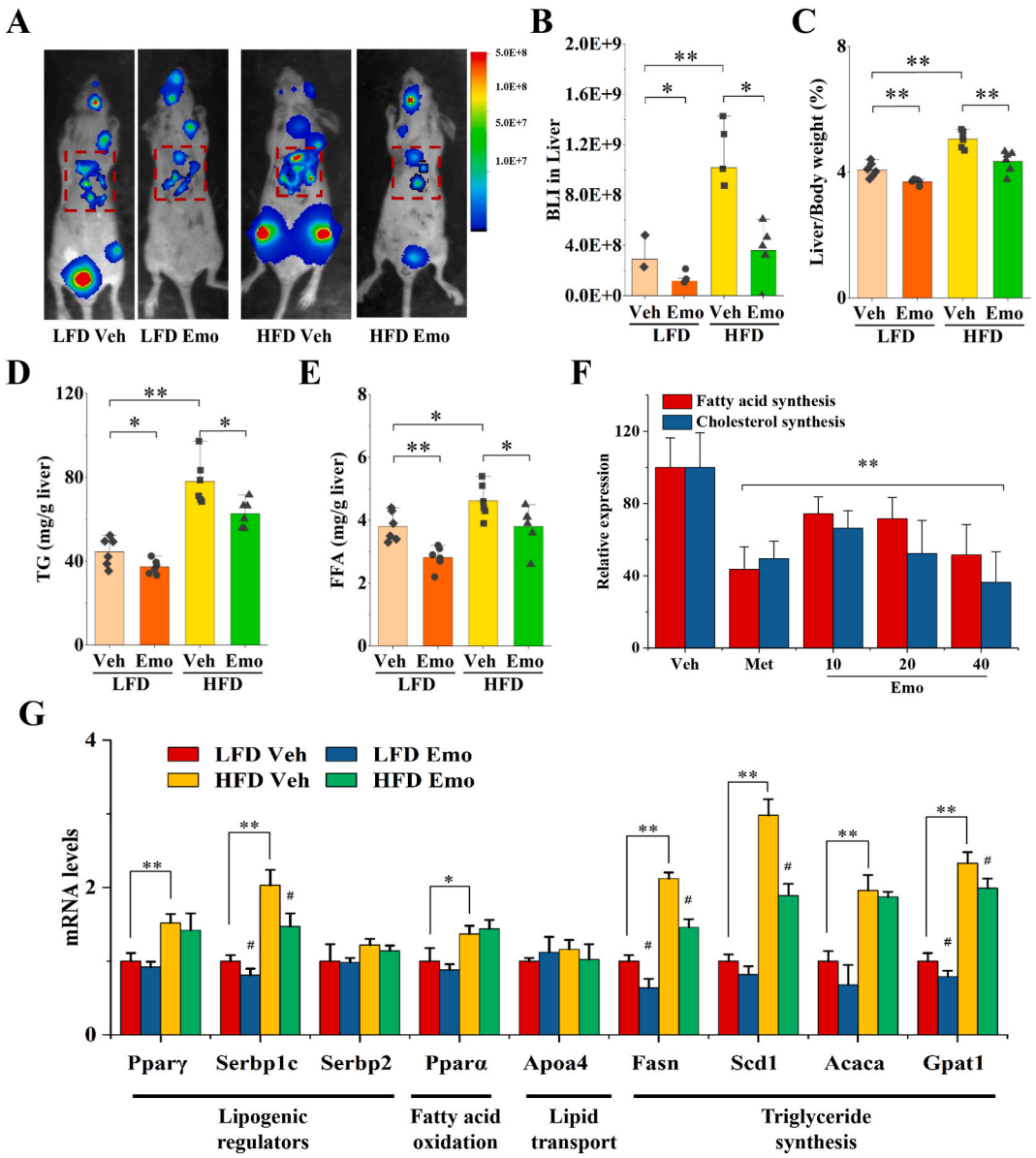

Fig. 5. Emodin inhibited breast cancer liver metastasis by regulating lipid synthesis in mice. Mice were fed a HFD or LFD for 9 weeks and were given an intravenous injection of luciferase-labeled MDA-MB-231 cells (4.0×10^6 cells/mouse) after anesthesia with pentobarbital sodium (50 mg/kg) (n = 6/group). The mice received emodin (400 mg/kg, p. o., q. d.) or vehicle for 4 weeks. For *in vivo* tumor proliferation, blood glucose and blood lipid detection in tumor-bearing mice, please refer to the Methods section. The means ± SDs with an asterisk (*) are significantly ($P < 0.05$) different from the vehicle. (A) Emodin attenuated breast cancer liver metastasis in mice. (B) Tumor proliferation in the liver of tumor-bearing mice. Effects of emodin on liver weight (C), liver TG (D), and liver FFA levels (E) in mice. (F) Emodin inhibited fatty acid synthesis and cholesterol synthesis in HepG2 cells. Three biological replicates were used for each treatment group. Metformin (Met) at a concentration of 1 mmol/L was used as a positive control. (G) Emodin reduced the lipogenic regulator Serbp1c and TG synthesis in the liver.

3.4. Emodin inhibited breast cancer liver metastasis in a mouse xenograft model

To explore the effects of emodin on breast cancer liver metastasis under the condition of obesity, mice were fed a HFD for 8 weeks before tumor injection. The HFD significantly increased body weight (Supplementary Figure 1A). Then, a mouse model of metastatic carcinoma was established by left ventricular injection. The body weight of the tumor-bearing mice was significantly reduced (Supplementary Figure 1A). HFD promoted breast cancer metastasis in mice, especially in the liver (Fig. 5A/B). Moreover, emodin significantly decreased liver metastasis of breast cancer after 4 weeks of treatment (Fig. 5A/B). Emodin also ameliorated glucose tolerance, especially under HFD conditions (Supplementary Figure 1B/C). In addition, emodin attenuated hyperglycemia and hyperinsulinemia induced by a HFD and ultimately improved insulin resistance (Supplementary Fig. 1D-F, Table 1). The levels of hepatic TGs and hepatic FFAs, but not hepatic TC, in the HFD group were higher than those in the LFD group (Fig. 5D/E and Supplementary Figure 1G). This situation may eventually result in a significant increase in liver weight in the HFD group compared with the LFD group (Fig. 5C). Interestingly, emodin decreased TG and FFA levels and ultimately reduced liver weight (Fig. 5C–E). This finding suggests that emodin significantly reduces the abnormal increase in liver weight induced by high-fat feeding, which may be due to the inhibition of liver lipid synthesis by emodin. Therefore, the regulation by emodin of the synthesis of fatty acids and cholesterol was investigated in hepatocytes. Emodin significantly inhibited fatty acid synthesis and cholesterol synthesis in HepG2 cells (Fig. 5F). In addition, HFD also promoted lipogenic regulator, fatty acid oxidation, and TG synthesis gene expression in the liver (Fig. 5G). Interestingly, emodin decreased the mRNA levels of the lipogenic regulator Serbp1c and reduced the expression of TG synthesis genes, such as Gpat1, Fasn, and Sed1, in the liver (Fig. 5G).

3.5. Emodin tightly bound to its target proteins

The interactions between emodin (Fig. 6A) and its target proteins were evaluated using molecular docking analysis. We found that emodin tightly bound to these candidate proteins, such as CSNK2A1, ESR, PIM1 and PTP4A3 (Fig. 6B–F). All of the binding affinities of the interactions were less than −8 kcal/mol (Fig. 6G).

3.6. Emodin regulated ERK/AKT signaling

Based on bioinformatics and the molecular docking results, we investigated the effect of emodin on the ERK and AKT signaling pathways. We found that emodin significantly reduced the phosphorylation levels of ERK1/2 and AKT but not p38 MAPK in MDA-MB-231 cancer cells (Fig. 6H, Supplementary material 1 and Supplementary Figure 2).

4. Discussion

In the present study, we found that obesity and hyperlipidemia caused by a HFD accelerated the liver metastasis of breast cancer. Interestingly, emodin attenuated breast cancer liver metastasis through the AKT and ERK signaling pathways by interacting with CK2α.

The levels of lipids (TGs, TC, and LDL-C) in patients with cancer cell metastasis are higher than those in patients without distant metastasis in breast cancer [32]. This finding indicates that high lipid levels may contribute to the metastasis of breast cancer. A previous study confirmed that extended and chronic exposure to an elevated lipid diet results in sustained activation of lipid synthesis-related genes, such as PPARα, and transcriptional activation of PPARα-responsive genes, which affect intermediary metabolism in the liver [33]. These metabolic changes, along with the antiapoptotic effects of PPARα activation, contribute to oxidative DNA damage and create favorable conditions for the colonization of breast cancer cells in the liver [8]. Lipids synthesized by hepatocytes provide energy for cancer cells or materials for cell membrane synthesis [32,33]. These lipids may further enhance the degree of breast cancer proliferation in liver metastases. We also found that high lipid levels increase the malignancy of breast cancer cells. The results of the present study are also consistent with previous work demonstrating that high lipid levels endow cancer cells with high potential migration and invasion and thus increase the risk of liver metastasis in breast cancer [11,12].

In addition, emodin inhibits hepatic lipid synthesis and attenuates high levels of serum lipids in obese mice induced by a HFD via SREBP-1 and SREBP-2 downregulation [15]. The results of the bioinformatics analysis in this study indicated that emodin regulated the metabolism of lipid signaling pathways. Indeed, emodin decreased elevated levels of lipids in serum and liver via the inhibition of fatty acid and cholesterol synthesis in obese mice induced by a HFD through regulating TG synthesis genes, such as Fasn, Scd1, and

Table 1
The effect of emodin on liver function and lipids in serum.

	LFD Veh	LFD Emo	HFD Veh	HFD Emo
TC (mM)	2.12 ± 0.36	1.62 ± 0.31*	3.22 ± 0.32##	2.30 ± 0.48**
TG (mM)	0.77 ± 0.15	0.62 ± 0.14	1.27 ± 0.28##	0.90 ± 0.20*
LDL-C (mM)	0.42 ± 0.07	0.36 ± 0.04	1.01 ± 0.10##	0.85 ± 0.10*
HDL-C (mM)	1.23 ± 0.12	1.17 ± 0.14	1.92 ± 0.27##	1.49 ± 0.41
AST (U/L)	147.33 ± 10.35	141.33 ± 13.85	219.67 ± 10.61##	171.33 ± 6.19**
ALT (U/L)	58.83 ± 9.33	60.00 ± 7.24	127.33 ± 24.02##	103.50 ± 4.72*

*p < 0.05, **p < 0.01 compared with the corresponding Veh group; #p < 0.05, ##p < 0.01 compared with the LFD Veh group. Six mice were used in each group.

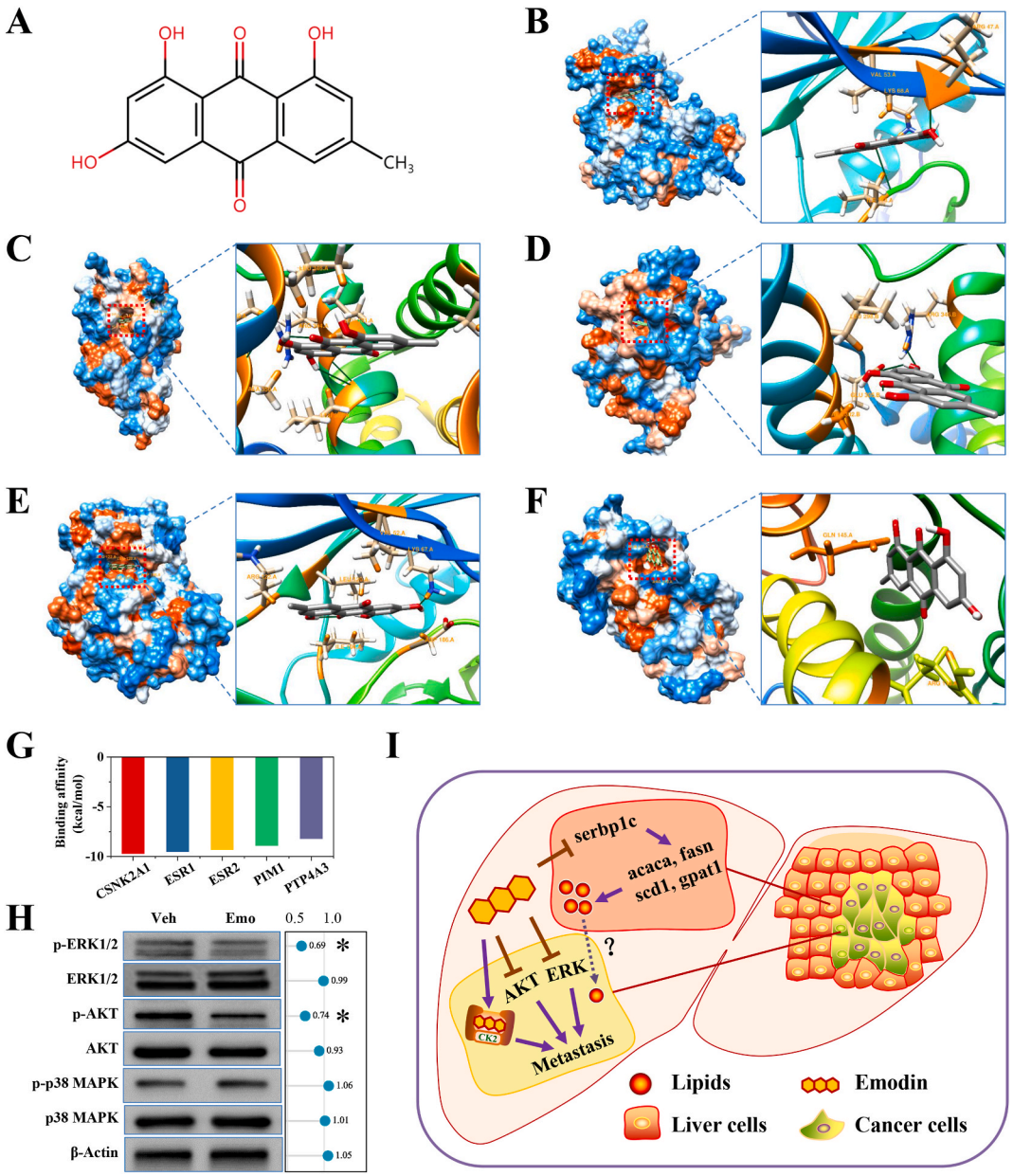

Fig. 6. Emodin regulated the ERK/AKT signaling pathway and interacted with CSNK2A1, ESR, PIM1 and PTP4A3. (A) The molecular structure of emodin. The binding action and binding site of emodin to CSNK2A1 (B), ESR1 (C), ESR2 (D), PIM1 (E) and PTP4A3 (F). (G) The results of the binding affinity between emodin and its targets. (H) Emodin decreased the phosphorylation levels of ERK1/2 and AKT, as shown by western blotting analysis. Three biological replicate was used for each treatment group. *p < 0.05 compared with the Veh group. (I) Schematic diagram of emodin inhibiting breast cancer liver metastasis.

Gpat1. Ketoconazole, an inhibitor of membrane sterol synthesis, can block carboxysterol dehydrogenase, a cholesterol synthase, and can thus prevent breast cancer metastasis [34]. This finding indicates that steroid biosynthesis may serve as a new drug target for breast cancer patients with liver metastasis. In addition, in the liver metastasis microenvironment of breast cancer, there are not only interactions between cancer cells and adipocytes but also interactions between cancer cells and other cells. For example, there are interactions between breast cancer cells and hepatocytes, immune cells or fibroblasts, and these interactions are also very important to the fate of breast cancer cells [24–26] This article not only objectively evaluated the efficacy of emodin in inhibiting liver metastasis of breast cancer but also explored the mechanism of emodin in inhibiting liver metastasis of breast cancer by using conditions closer to the clinical microenvironment of breast cancer liver metastasis. We found that inhibiting liver lipid synthesis may be one of the mechanisms by which emodin inhibits liver metastasis of breast cancer, especially in obese patients with breast cancer.

CK2α, a constitutively active, ubiquitous serine/threonine kinase, is elevated in every cancer type evaluated to date [35], including

breast cancer [36]. Overexpression of CK2α in the mammary gland of transgenic mice causes 32% of female MMTV-CK2α transgenic mice to develop mammary adenocarcinomas at a median of 23 months of age [37]. A previous study confirmed that inhibition of CK2α caused a range of phenotypic changes in breast cancer cells, including decreased breast cancer cell viability, cell cycle arrest, apoptosis, and loss of migratory capacity [38]. Treatments with CK2α inhibitors, such as CX-4945 and TBB, could inhibit the PI3K/Akt/mTOR, nuclear factor kappa-B (NF-κB), signal transducer and activator of transcription 3 (STAT3) pathways in MDA-MB-231 and MCF-7 cells [37]. Bioinformatics prediction analysis found that emodin could regulate the CK2α, AHR, and ALDH3A2 genes. We also found that emodin interacted with CK2α and inhibited the AKT and ERK signaling pathways in breast cancer cells. These results demonstrate the potential of CK2α as a clinical target in breast cancer. Additionally, emodin also decreased the proliferation and invasiveness of breast cancer cells. These studies were consistent with previous work indicating that emodin attenuates breast cancer cell metastasis and angiogenesis via MMPs, VEGFR, and EMT inhibition [22,23]. The inhibition of breast cancer cells through the AKT and ERK pathways via interaction with CK2α may be another one of the mechanisms by which emodin inhibits liver metastasis in breast cancer.

Although the pathological diagnosis of our previous study confirmed the inhibitory effect of emodin on liver metastasis [23], the pathological diagnosis of liver metastasis in this article was lacking. This study can more objectively evaluate the inhibitory effect and mechanism of emodin on liver metastasis based on the regulatory effects of various factors in the liver metastatic microenvironment of breast cancer cells.

5. Conclusion

Although the mechanism by which emodin regulates the absorption and utilization of hepatic lipid synthesis by breast cancer cells remains unclear, our study provides direct evidence for the attenuation by emodin of the high metastatic potential to the liver in the state of obesity and hyperlipidemia induced by a HFD through the AKT and ERK signaling pathways interacting with CK2α in breast cancer (Fig. 6I).

Declarations

Author contribution statement

Feng Li; Xiaoyun Song: Performed the experiments, Analyzed and interpreted the data, Wrote the paper.
Xiqiu Zhou; Lili Chen: Analyzed and interpreted the data, Contributed reagents, materials, analysis tools or data.
Jinzhou Zheng: Conceived and designed the experiments, Wrote the paper.

Funding statement

This research was supported by The Research and Cultivation Plan of Longhua Hospital (No. LYTD-58).

Data availability

The datasets used and/or analyzed during this study are available from the corresponding author on reasonable request.

Ethics approval

All experiments were approved by the Institutional Animal Care and Use Committee (IACUC) of Longhua Hospital with approval number 2019-N009.

All methods were carried out according to the guidelines and regulations for animal experimentation and were approved by the IACUC of Longhua Hospital. All methods are reported in compliance with the ARRIVE guidelines (https://arriveguidelines.org) for the reporting of animal experiments.

Declaration of competing interest

The authors declare that they have no known competing financial interests or personal relationships that could have appeared to influence the work reported in this paper.

Appendix A. Supplementary data

Supplementary data related to this article can be found at https://doi.org/10.1016/j.heliyon.2023.e17052.

References

[1] R.L. Siegel, K.D. Miller, H.E. Fuchs, et al., Cancer statistics, 2021. CA, Cancer J Clin 71 (1) (2021) 7–33.
[2] E. Fuentes-Mattei, G. Velazquez-Torres, L. Phan, et al., Effects of obesity on transcriptomic changes and cancer hallmarks in estrogen receptor–positive breast cancer, J. Natl. Cancer Inst. 6 (7) (2014) dju158, pii.
[3] D.S. Chan, A.R. Vieira, D. Aune, et al., Body mass index and survival in women with breast cancer-systematic literature review and meta-analysis of 82 follow-up studies, Ann. Oncol. 25 (10) (2014) 1901–1914.
[4] A.H. Eliassen, G.A. Colditz, B. Rosner, et al., Adult weight change and risk of postmenopausal breast cancer, JAMA 296 (2) (2006) 193–201.
[5] M. Ewertz, M.-B. Jensen, K.Á. Gunnarsdóttir, et al., Effect of obesity on prognosis after early-stage breast cancer, J. Clin. Oncol. 29 (1) (2011) 25–31.
[6] W. Wu, J. Chen, W. Ye, et al., Fatty liver decreases the risk of liver metastasis in patients with breast cancer: a two-center cohort study, Breast Cancer Res. Treat. 166 (1) (2017) 289–297.
[7] A.O. Duran, A. Yildirim, M. Inanc, et al., Hepatic steatosis is associated with higher incidence of liver metastasis in patients with metastatic breast cancer; an observational clinical study, J BUON 20 (4) (2015) 963–969.
[8] Y. Li, X. Su, N. Rohatgi, et al., Hepatic lipids promote liver metastasis, JCI Insight 5 (17) (2020), e136215.
[9] Y.Y. Wang, C. Attané, D. Milhas, et al., Mammary adipocytes stimulate breast cancer invasion through metabolic remodeling of tumor cells, JCI Insight 2 (4) (2017), e87489.
[10] C.H. Yao, R. Fowle-Grider, N.G. Mahieu, et al., Exogenous fatty acids are the preferred source of membrane lipids in proliferating fibroblasts, Cell Chem. Biol. 23 (4) (2016) 483–493.
[11] J.W. Lee, M.L. Stone, P.M. Porrett, et al., Hepatocytes direct the formation of a pro-metastatic niche in the liver, Nature 567 (7747) (2019) 249–252.
[12] Z. Madak-Erdogan, S. Band, Y.C. Zhao, et al., Free fatty acids rewire cancer metabolism in obesity-associated breast cancer via estrogen receptor and mTOR signaling, Cancer Res. 79 (10) (2019) 2494–2510.
[13] X. Dong, J. Fu, X. Yin, et al., Emodin: a review of its pharmacology, toxicity and pharmacokinetics, Phytother Res. 30 (8) (2016) 1207–1218.
[14] Z. Chen, L. Zhang, J. Yi, et al., Promotion of adiponectin multimerization by emodin: a novel AMPK activator with PPARγ-agonist activity, J. Cell. Biochem. 113 (11) (2012) 3547–3558.
[15] J. Li, L. Ding, B. Song, et al., Emodin improves lipid and glucose metabolism in high fat diet-induced obese mice through regulating SREBP pathway, Eur. J. Pharmacol. 770 (2016) 99–109.
[16] P. Song, J.H. Kim, J. Ghim, et al., Emodin regulates glucose utilization by activating AMP-activated protein kinase, J. Biol. Chem. 288 (8) (2013) 5732–5742.
[17] M. Zhou, H. Xu, L. Pan, et al., Emodin promotes atherosclerotic plaque stability in fat-fed apolipoprotein E-deficient mice, Tohoku J. Exp. Med. 215 (1) (2008) 61–69.
[18] X. Jia, S. Iwanowycz, J. Wang, et al., Emodin attenuates systemic and liver inflammation in hyperlipidemic mice administrated with lipopolysaccharides, Exp. Biol. Med.: Maywood 239 (8) (2014) 1025–1035.
[19] S. Wang, X. Li, H. Guo, et al., Emodin alleviates hepatic steatosis by inhibiting sterol regulatory element binding protein 1 activity by way of the calcium/calmodulin-dependent kinase kinase-AMP-activated protein kinase–mechanistic target of rapamycin-p70 ribosomal S6 kinase signaling pathway, Hepatol. Res. 47 (7) (2016) 683–701.
[20] P.H. Huang, C.Y. Huang, M.C. Chen, et al., Emodin and aloe-emodin suppress breast cancer cell proliferation through ERα inhibition, Evid. Base Compl. Alternative Med. (2013), 376123.
[21] C. Zu, M. Zhang, H. Xue, et al., Emodin induces apoptosis of human breast cancer cells by modulating the expression of apoptosis-related genes, Oncol. Lett. 10 (5) (2015) 2919–2924.
[22] J. Ma, H. Lu, S. Wang, et al., The anthraquinone derivative emodin inhibits angiogenesis and metastasis through downregulating Runx2 activity in breast cancer, Int. J. Oncol. 46 (4) (2015) 1619–1628.
[23] X. Song, X. Zhou, Y. Qin, et al., Emodin inhibits epithelial-mesenchymal transition and metastasis of triple negative breast cancer via antagonism of CC-chemokine ligand 5 secreted from adipocytes, Int. J. Mol. Med. 42 (1) (2018) 579–588.
[24] M. Boieri, A. Malishkevich, R. Guennoun, et al., CD4+ T helper 2 cells suppress breast cancer by inducing terminal differentiation, J. Exp. Med. 219 (7) (2022), e20201963.
[25] D. Hu, Z. Li, B. Zheng, et al., Cancer-associated fibroblasts in breast cancer: challenges and opportunities, Cancer Commun. 42 (5) (2022) 401–434.
[26] S.Z. Wu, D.L. Roden, C. Wang, et al., Stromal cell diversity associated with immune evasion in human triple-negative breast cancer, EMBO J. 39 (19) (2020), e104063.
[27] T. Obsen, N.J. Faergeman, S. Chung, et al., Trans-10, cis-12 conjugated linoleic acid decreases de novo lipid synthesis in human adipocytes, J. Nutr. Biochem. 23 (6) (2012) 580–590.
[28] X. Gao, Z. Yang, C. Xu, et al., GeneChip expression profiling identified OLFML2A as a potential therapeutic target in TNBC cells, Ann. Transl. Med. 10 (6) (2022) 274.
[29] M. Chen, C. Wu, Z. Fu, S. Liu, ICAM1 promotes bone metastasis via integrin-mediated TGF-β/EMT signaling in triple-negative breast cancer, Cancer Sci. 113 (11) (2022) 3751–3765.
[30] J. Ding, Z. Liang, W. Feng, et al., Integrated bioinformatics analysis reveals potential pathway biomarkers and their interactions for clubfoot, Med. Sci. Mon. Int. Med. J. Exp. Clin. Res. 26 (2020), e925249.
[31] M.F. Isaac-Lam, Molecular modeling of the interaction of ligands with ACE2-SARS-CoV-2 spike protein complex, Silicon Pharmacol. 9 (1) (2021) 55.
[32] L. Shuai, L.L. Zhang, Predictive value of blood lipids for distant metastasis of breast cancer, Smart Healthc. 3 (9) (2017) 5–9.
[33] S.R. Pyper, N. Viswakarma, S. Yu, et al., PPARα: energy combustion, hypolipidemia, inflammation and cancer, Nucl. Recept. Signal. 8 (1) (2010), e002.
[34] M. Chen, Y. Zhao, X. Yang, et al., NSDHL promotes triple-negative breast cancer metastasis through the TGFβ signaling pathway and cholesterol biosynthesis, Breast Cancer Res. Treat. 187 (2021) 349–362.
[35] M. Ruzzene, L.A. Pinna, Addiction to protein kinase CK2: a common denominator of diverse cancer cells? Biochim. Biophys. Acta 1804 (3) (2010) 499–504.
[36] J.S. Bae, S.H. Park, U. Jamiyandorj, et al., CK2a/CSNK2A1 phosphorylates SIRT6 and is involved in the progression of breast carcinoma and predicts shorter survival of diagnosed patients, Am. J. Pathol. 186 (12) (2016) 3297–3315.
[37] E. Landesman-Bollag, R. Romieu-Mourez, D.H. Song, et al., Protein kinase CK2 in mammary gland tumorigenesis, Oncogene 20 (25) (2001) 3247–3257.
[38] G.K. Gray, B.C. McFarland, A. Rowse, et al., Therapeutic CK2 inhibition attenuates diverse prosurvival signaling cascades and decreases cell viability in human breast cancer cells, Oncotarget 5 (15) (2014) 6484–6496.